ACS APPLIED MATERIALS & INTERFACES

Research Article

www.acsami.org

Phosphine Oxide Type Bipolar Host Material for High Quantum Efficiency in Thermally Activated Delayed Fluorescent Device

Bo Seong Kim and Jun Yeob Lee*

Department of Polymer Science and Engineering, Dankook University Jukjeon-dong, Suji-gu, Yongin-si, Gyeonggi-do 448-701, Korea

ABSTRACT: Highly efficient thermally activated delayed fluorescence devices were developed using a bipolar host material, 2,7-bis-(diphenylphosphoryl)-9-phenyl-9H-carbazole (PPO27), derived from carbazole and diphenylphosphine oxide. The PPO27 host was effective for good charge balance and energy transfer from the PPO27 host to thermally activated delayed fluorescence dopant. The PPO27 device doped with (4s,6s)-2,4,5,6-tetra(9H-carbazol-9-yl)isophthalonitrile dopant could realize a high quantum efficiency of 24.2%.

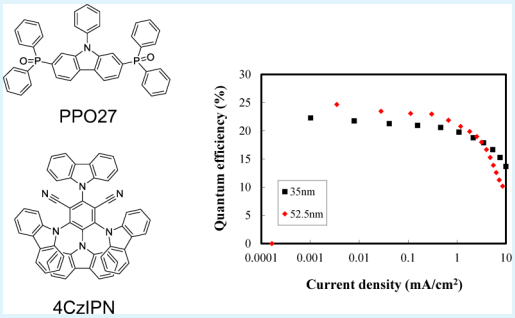

KEYWORDS: *thermally activated delayed fluorescence, bipolar host, phosphine oxide, green fluorescent device*

INTRODUCTION

Recently, thermally activated delayed fluorescence (TADF) devices have gained much interest due to theoretical internal quantum efficiency of 100%.[1] Common fluorescent organic light-emitting diodes (OLEDs) can reach a theoretical internal quantum efficiency of 25%,[2−4] but the TADF OLEDs can show four times higher quantum efficiency due to singlet harvesting by reverse intersystem crossing. Triplet exciton conversion from triplet state to singlet state can occur via intersystem crossing and can contribute to fluorescent emission.

There have been several works studying TADF OLEDs to for better quantum efficiency in fluorescent OLEDs.[5−12] Adachi et al. reported several TADF emitting materials with an emission wavelength from orange to sky blue. The most efficient TADF emitter was (4s,6s)-2,4,5,6-tetra(9H-carbazol-9-yl)isophthalonitrile (4CzIPN) and the 4CzIPN doped device could allow high quantum efficiency of 19.3% in green TADF OLEDs.[1] High photoluminescence (PL) quantum yield of 94 ± 2% was the origin for the high quantum efficiency of the 4CzIPN device. However, the device performances of the 4CzIPN could not be optimized because hole transport type 4,4′-bis(carbazol-9-yl)biphenyl (CBP) was the host material. In spite of the high triplet energy of CBP (2.56 eV), the hole transport character of CBP could not increase the quantum efficiency of the 4CzIPN device.[13−15] In addition, the low triplet energy of 4,4-bis[N-(1-naphthyl)-*N*-phenylamino]-biphenyl also quenched triplet excitons of 4CzIPN and decreased the quantum efficiency of the 4CzIPN TADF OLEDs.[16] Therefore, the device structure 4CzIPN devices needs to be optimized to enhance the quantum efficiency. In our previous work, we reported furodipyridine derived materials as the host materials for the 4CzIPN dopant.[17] However, the furodipyridine type materials formed exciplex with 4CzIPN because of diphenylamine moiety, which restricted the quantum efficiency of the 4CzIPN device despite of bipolar character. The exciplex formation could be avoided using a bipolar host material derived from carbazole in other works.[18,19] Therefore, carbazole based host materials with electron withdrawing substituents would be ideal as the host materials for 4CzIPN.

In this work, a bipolar type host, 2,7-bis-(diphenylphosphoryl)-9-phenyl-9H-carbazole (PPO27), was applied in the 4CzIPN device for high recombination efficiency without exciplex formation and an exciton confining device architecture was designed to confine both singlet and triplet excitons. Herein, we describe that the PPO27 host is useful for high quantum efficiency in the 4CzIPN device by demonstrating quantum efficiency of 24.2% after optimizing the device structure.

EXPERIMENTAL SECTION

The TADF OLED structure was indium tin oxide (ITO, 50 nm)/poly(3,4-ethylenedioxythiophene):poly(styrenesulfonate) (PEDOT:PSS, 60 nm)/4,4′-cyclohexylidenebis[*N*,*N*-bis(4-methylphenyl)-aniline] (TAPC, 20 nm)/1,3-bis(N-carbazolyl)benzene (mCP, 10 nm)/PPO27:4CzIPN (25 nm, 1 or 2 or 5%)/diphenylphosphine oxide-4-(triphenylsilyl)phenyl (TSPO1, 35 nm)/LiF(1 nm)/Al(200 nm). The thickness of the TSPO1 layer was controlled for optimized device performances in the PPO27 TADF OLEDs. The thicknesses of the TSPO1 electron transport layer were 35 and 52.5 nm. Chemical structures of PPO27 and 4CzIPN are presented in Figure 1. The TADF OLEDs were fabricated by vacuum evaporation and the evaporation was carried out at a rate of 0.1 nm/s except for the 4CzIPN dopant. The TADF OLEDs were encapsulated for device performance measurement in air. A Keithley 2400 source measurement unit was used for the measurement of current density (J)−voltage (V) characteristics, and a CS2000 spectroradiometer was used

Received: March 4, 2014
Accepted: April 16, 2014
Published: April 28, 2014

   dx.doi.org/10.1021/am501301g | *ACS Appl. Mater. Interfaces* 2014, 6, 8396−8400

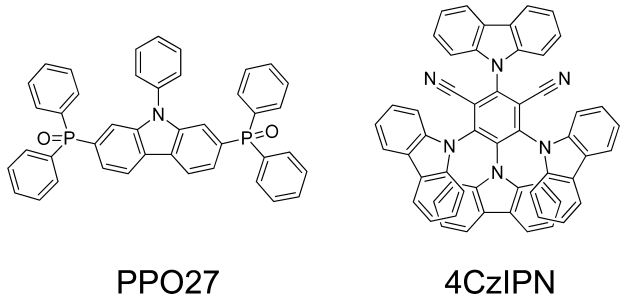

Figure 1. Chemical structures of PPO27 and 4CzIPN.

to measure luminance (L) and emission spectra. Light emission perpendicular to the substrate was measured, and Lambertian distribution of light emission was assumed to calculate the quantum efficiency.

RESULTS AND DISCUSSION

PPO27 has been known as a host material with a singlet/triplet energy of 3.16/2.81 eV and bipolar charge transport character.[20] The high singlet and triplet energies of PPO27 made it suitable for application in blue phosphorescent OLEDs via efficient singlet and triplet energy transfer. Additionally, the bipolar charge transport character of PPO27 optimized charge balance and upgraded the efficiency of sky blue phosphorescent OLEDs. Therefore, PPO27 can also be applied as the matrix for 4CzIPN with a singlet/triplet energy of 2.46/2.37 eV.

In order to analyze the energy transfer from PPO27 to 4CzIPN, PL emission spectrum of PPO27 and ultraviolet−visible (UV−vis) absorption spectrum of 4CzIPN were compared. Figure 2 represents UV−vis spectrum of 4CzIPN

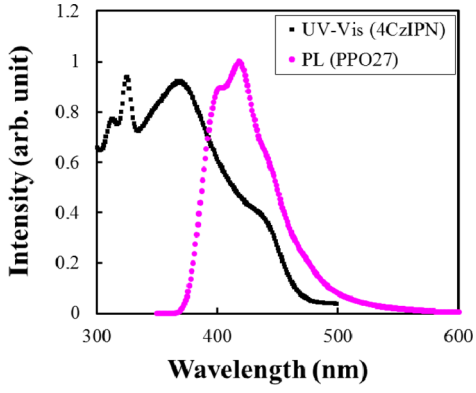

Figure 2. UV−vis absorption of 4CzIPN and PL emission of PPO27.

and PL emission spectrum of PPO27. There was extensive overlap between PL emission of PPO27 centered at 392 nm and UV−vis absorption of 4CzIPN. The extensive spectral overlap between the PL spectrum of PPO27 and UV−vis absorption of 4CzIPN implies that PPO27 would transfer emission energy to 4CzIPN.

The PL emission of PPO27:4CzIPN was further investigated according to doping concentration of 4CzIPN. PL spectra of PPO27:4CzIPN were measured at different doping concentrations of 4CzIPN, which is shown in Figure 3a. Strong PL emission peak corresponding to the emission of 4CzIPN was observed between 498 and 509 nm depending on the doping concentration of 4CzIPN and weak PPO27 emission was observed at 392 nm. Comparing the PL emission of PPO27:4CzIPN, the PL emission of PPO27:4CzIPN was

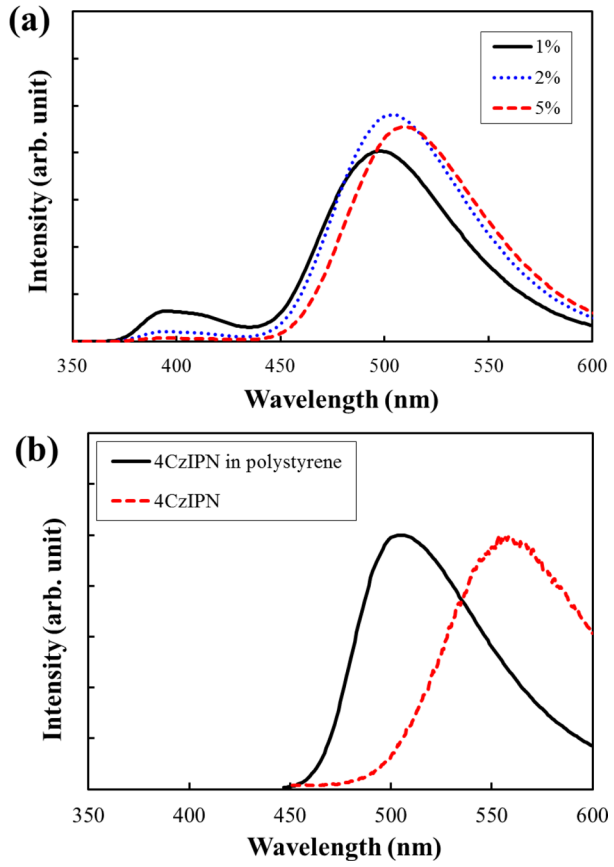

Figure 3. Solid PL spectra of PPO27:4CzIPN film at different doping concentrations (a) and PL spectra of pure 4CzIPN and 4CzIPN dispersed in polystyrene (b). Excitation wavelength was 310 nm.

intensified at 2% 4CzIPN concentration and it was weakened at 1% and 5% 4CzIPN concentrations. The weak PPO27 emission at 2% doping concentration suggests incomplete energy transfer from PPO27 to 4CzIPN at 2% 4CzIPN concentration. However, the PL emission was maximized at 2% doping concentration even though PPO27 emission was suppressed at 5% doping concentration. This behavior can be explained by strong intermolecular interaction of the 4CzIPN dopant in the PPO27 host. Although the energy transfer was efficient at 5% doping concentration, concentration quenching effect is serious due to highly polar molecular structure, which is supported by the red shift of the PL emission peak by 11 nm, resulting in reduced PL intensity. PL spectra of 4CzIPN dispersed in polystyrene and pure 4CzIPN film are shown in Figure 3b to confirm that the red-shift is due to intermolecular interaction. At 1% doping concentration, incomplete energy transfer decreased the PL intensity as can be seen in the strong PPO27 host emission in the PL spectrum. Therefore, the energy transfer from PPO27 to 4CzIPN is improved and the concentration quenching effect is not significant at 2% doping concentration. It can be inferred from the PL data that the quantum efficiency may be boosted if the device structure can be optimized at 2% 4CzIPN concentration.

TADF behavior of the PPO27:4CzIPN emitting layer was investigated by monitoring the PL emission of PPO27:4CzIPN after applying delay time of 1 μs for PL measurement. Figure 4 compares PL spectra of PPO27:4CzIPN (2% doping) with and without applying delay time. The PL spectra were normalized to compare the PL emission pattern with and without delay

dx.doi.org/10.1021/am501301g | ACS Appl. Mater. Interfaces 2014, 6, 8396−8400

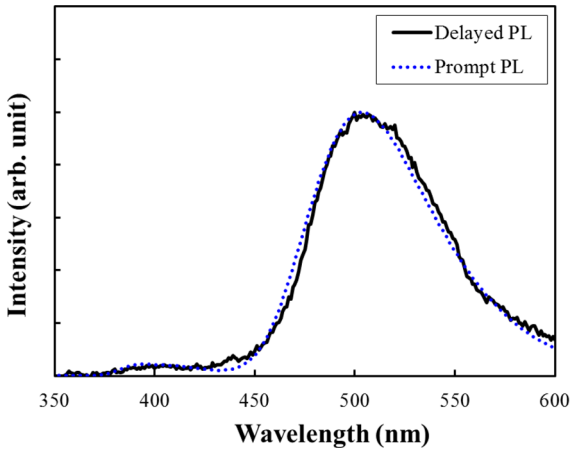

Figure 4. Prompt and delayed PL spectra of PPO27:4CzIPN film. Delay time was 1 μs and doping concentration of 4CzIPN was 2%.

time. There was little difference of the PL emission with and without delay time, indicating that the PL emission after delay time is TADF emission of 4CzIPN dopant. The TADF emission of 4CzIPN has an excited state lifetime of 5.1 μs, but fluorescent emission of 4CzIPN has the excited state lifetime of 17.8 ns.[1] Therefore, the delayed emission is caused by delayed fluorescence, confirming TADF emission of PPO27:4CzIPN emitting layer. The PPO27 host harvested the triplet excitons of 4CzIPN for singlet emission through TADF process.

The TADF emission of 4CzIPN in the PPO27 host was further confirmed by transient PL measurement of PPO27:4CzIPN. Transient PL data of PPO27:4CzIPN film are presented in Figure 5. Single decay curve of the delayed emission of

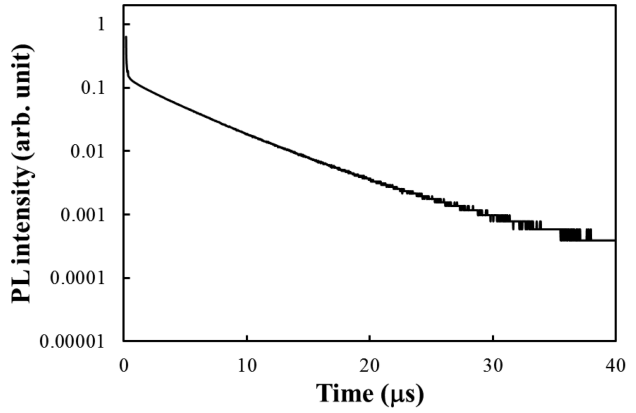

Figure 5. Transient PL decay curve of PPO27:4CzIPN film. Doping concentration of 4CzIPN was 2%.

4CzIPN was observed and the excited state lifetime for the TADF emission was 4.3 μs. There was little difference of the excited state lifetime between PPO27:4CzIPN and 4CzIPN, implying efficient energy transfer from PPO27 to 4CzIPN and effective activation of TADF emission of 4CzIPN.

As PPO27 exhibited photophysical properties appropriate for application as the host material for 4CzIPN, green TADF OLEDs were fabricated by using the PPO27:4CzIPN emitting layer. The PPO27:4CzIPN devices were constructed to confine both singlet and triplet excitons in the emitting layer without exciton quenching or charge leakage. The mCP hole transport material possesses the highest occupied molecular orbital (HOMO) of −6.1 eV, the lowest unoccupied molecular orbital (LUMO) of −2.4 eV and a high singlet/triplet energy of 3.46/2.90 eV. 4CzIPN possessed the HOMO/LUMO level of −5.80/−3.40 eV,[21] and it is expected that the deep HOMO and shallow LUMO of mCP suppresses exciton quenching and charge leakage. The high triplet energy of mCP also prevents triplet exciton quenching of 4CzIPN by mCP. Similarly, the HOMO/LUMO level (−6.79/−2.52 eV) and high triplet energy (3.36 eV) of TSPO1 confine excitons of 4CzIPN in the emitting layer.[22] Figure 6 shows J−V−L data of PPO27:4C-

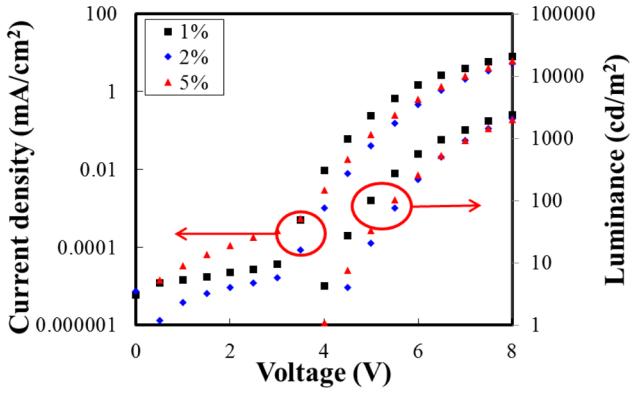

Figure 6. Current density−voltage−luminance curves of PPO27:4CzIPN devices with different 4CzIPN doping concentrations.

zIPN devices at different doping concentrations of 4CzIPN. The J of the PPO27:4CzIPN devices is lowered by doping up to 2% and then rises again at 5%. The low J at 2% is caused by charge trapping effect by 4CzIPN. Compared with the 1% 4CzIPN doped device, more charges are trapped by 4CzIPN, lowering the current density at 2%. The HOMO and LUMO differences between PPO27 and 4CzIPN are 0.45 and 0.40 eV, respectively. The large energy level gap between PPO27 and 4CzIPN induces carrier trapping by 4CzIPN and the low J. The reduced J is increased at 5% because of facilitated charge hopping via the 4CzIPN dopant.

Quantum efficiency of the PPO27:4CzIPN devices is plotted against current density in Figure 7. Optimum doping concentration for the quantum efficiency of the PPO27:4CzIPN devices is 2%, and the maximum quantum efficiency is 21.1%, which is much higher than 16.6% of the CBP:4CzIPN device. Even though 19.3% quantum efficiency was reported in

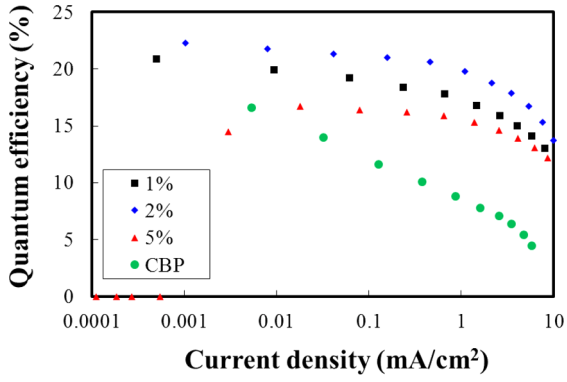

Figure 7. Quantum efficiency−luminance curves of PPO27:4CzIPN devices with different 4CzIPN doping concentrations. Device performances of CBP:4CzIPN device was added for comparison.

dx.doi.org/10.1021/am501301g | ACS Appl. Mater. Interfaces 2014, 6, 8396−8400

Table 1. Device Performances of the PPO27:4CzIPN OLEDs

		quantum efficiency [%]			power efficiency [lm W^{1-}]		
doping concn./TSPO1 thickness	color index[a]	max	100 [cd m^{-2}]	1000 [cd m^{-2}]	max	100 [cd m^{-2}]	1,000 [cd m^{-2}]
1%/35 nm	0.19, 0.45	20.3 ± 0.5	18.4 ± 0.1	15.8 ± 0.1	42.1 ± 0.2	29.1 ± 0.2	18.9 ± 0.2
2%/35 nm	0.19, 0.46	21.1 ± 0.6	20.2 ± 0.7	18.1 ± 0.6	42.1 ± 2.2	28.9 ± 1.2	20.2 ± 0.9
5%/35 nm	0.22, 0.51	16.0 ± 0.7	15.7 ± 0.5	14.2 ± 0.3	30.8 ± 1.9	25.2 ± 0.8	17.5 ± 0.4
2%/52.5 nm	0.20, 0.48	24.2 ± 0.5	22.7 ± 2.0	19.2 ± 0.3	52.0 ±	36.6 ± 0.7	22.0 ± 0.4

[a]Color index was obtained at 100 cd m^{-2}.

the CBP:4CzIPN device,[1] the same device performances could not be realized even after device optimization using a charge confining device structure. The enhanced device performances of the PPO27:4CzIPN device are attributed to the charge confining stack structure and bipolar character of PPO27. Singlet and triplet excitons of 4CzIPN are entrapped in the PPO27:4CzIPN emitting layer because mCP and TSPO1 charge transport materials have high singlet and triplet energies for exciton confinement and the appropriate energy levels for charge confinement. In addition, PPO27 can also limit exciton quenching due to high singlet and triplet energies. Therefore, excitons can be effectively used for light emission with little quenching by host and charge transport materials. The bipolar charge transport character of PPO27 balancing holes and electrons contributes to the high quantum efficiency.[20] The hole mobility of PPO27 was 8×10^{-5} cm^2 V^{-1} s^{-1} and electron mobility was 7×10^{-6} cm^2 V^{-1} s^{-1}. The charge balance improves exciton formation efficiency and enhancing the quantum efficiency of the PPO27 device. In addition, the efficient energy transfer from the host to dopant improves the quantum efficiency of the PPO27:4CzIPN TADF OLEDs. The low efficiency at 1% is caused by relatively poor energy transfer and the low efficiency at 5% is originated from reduced PL intensity caused by exciton quenching at high doping concentration. Device performances of the PPO27:4CzIPN devices are listed in Table 1.

Figure 8 exhibits electroluminescence (EL) spectra of the PPO27:4CzIPN devices. Strong EL emission of 4CzIPN

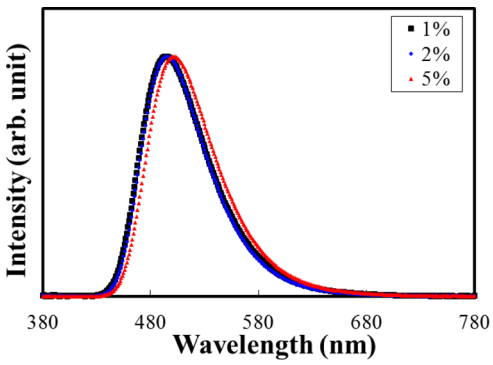

Figure 8. EL spectra of PPO27:4CzIPN devices with different 4CzIPN doping concentrations.

appears at 492 nm, but weak additional emission around 390 nm is observed in the PPO27:4CzIPN device at 1% owing to poor energy transfer from PPO27 to 4CzIPN. The PPO27 emission is not observed in other devices. Additionally, strong intermolecular interaction at high doping concentrations gave rise to long wavelength shift of the EL emission. Color coordinate of the green TADF OLEDs is not greatly affected by the doping concentration. The PPO27:4CzIPN device doped with 2% 4CzIPN demonstrates a color coordinate of (0.19,0.45) at 1000 cd/m^2.

The device performances of the TADF OLEDs are further upgraded by adjusting the thickness of the TSPO1 layer. The TSPO1 layer is thickened to 52.5 nm for better charge balance in the device.

Quantum efficiency−L performances of the PPO27:4CzIPN device with different TSPO1 thicknesses are represented in Figure 9. The maximum quantum efficiency of the

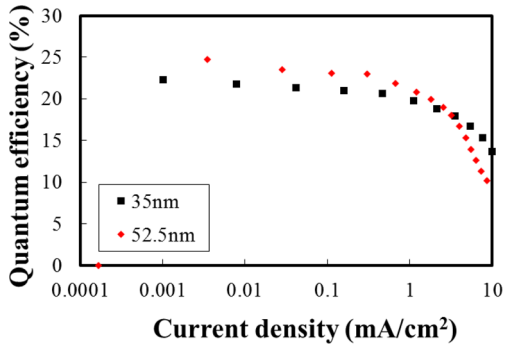

Figure 9. Quantum efficiency−luminance curves of PPO27:4CzIPN devices with different electron transport layer thicknesses.

PPO27:4CzIPN device is 24.2%. The quantum efficiency is decreased at 1000 cd/m^2, and the quantum efficiency at 1000 cd/m^2 is 19.2%. There was 13% improvement of the quantum efficiency after optimizing the thickness of the TSPO1 layer possibly due to better charge balance. However, the lifetime of the device was very short due to poor stability of the host and charge transport materials and further development of stable host materials will follow to improve the lifetime of the TADF devices.

CONCLUSIONS

High quantum efficiency green TADF OLEDs were developed by doping 4CzIPN in the PPO27 host. The quantum efficiency of the PPO27:4CzIPN device was enhanced up to 24.2% by devising as device architecture to optimize energy transfer, charge balance, and exciton blocking. Therefore, bipolar host materials are useful as the host for the TADF dopant material and the device performance of the green TADF OLEDs can be comparable to that of green phosphorescent OLEDs by optimizing the host materials and device architecture of the TADF OLEDs.

AUTHOR INFORMATION

Corresponding Author

*Tel: 82-31-8005-3585. Fax:82-31-8005-3585. E-mail: leej17@dankook.ac.kr.

Notes

The authors declare no competing financial interest.

REFERENCES

(1) Uoyama, H.; Goushi, K.; Shizu, K.; Nomura, H.; Adachi, C. Highly Efficient Organic Light-Emitting Diodes from Delayed Fluorescence. *Nature* **2012**, *492*, 234−238.

(2) Pope, M.; Kallmann, H. P.; Magnante, P. Electroluminescence in Organic Crystals. *J. Chem. Phys.* **1963**, *38*, 2042.

(3) Zhen, C.; Dai, Y.; Zeng, W.; Ma, Z.; Chen, Z.; Kieffer, J. Achieving Highly Efficient Fluorescent Blue Organic Light-Emitting Diodes Through Optimizing Molecular Structures and Device Configuration. *Adv. Funct. Mater.* **2011**, *21*, 699−707.

(4) Wei, Y.; Chen, C. T. Doubly Ortho-Linked cis-4,4′-Bis-(diarylamino)stilbene/Fluorene Hybrids as Efficient Nondoped, Sky-Blue Fluorescent Materials for Optoelectronic Applications. *J. Am. Chem. Soc.* **2007**, *129*, 7478−7479.

(5) Dias, F. B.; Bourdakos, K. N.; Jankus, V.; Moss, K. C.; Karntekar, K. T.; Bhalla, V.; Santos, J.; Bryce, M. R.; Monkman, A. P. Triplet Harvesting with 100% Efficiency by Way of Thermally Activated Delayed Fluorescence in Charge Transfer OLED Emitters. *Adv. Mater.* **2013**, *25*, 3707−3714.

(6) Goushi, K.; Yoshida, K.; Sato, K.; Adachi, C. Organic Light-Emitting Diodes Employing Efficient Reverse Intersystem Crossing for Triplet-to-Singlet State Conversion. *Nat. Photonics* **2012**, *6*, 253−258.

(7) Zhang, Q.; Li, J.; Shizu, K.; Huang, S.; Hirata, S.; Miyazaki, H.; Adachi, C. Design of Efficient Thermally Activated Delayed Fluorescence Materials for Pure Blue Organic Light Emitting Diodes. *J. Am. Chem. Soc.* **2012**, *134*, 14706−14709.

(8) Li, J.; Nakagawa, T.; Zhang, Q.; Nomura, H.; Miyazaki, H.; Adachi, C. Highly Efficient Organic Light-Emitting Diode Based on a Hidden Thermally Activated Delayed Fluorescence Channel in a Heptazine Derivative. *Adv. Mater.* **2013**, *25*, 3319−3323.

(9) Lee, S. Y.; Yasuda, T.; Nomura, H.; Adachi, C. High-Efficiency Organic Light-Emitting Diodes Utilizing Thermally Activated Delayed Fluorescence from Triazine-Based Donor−Acceptor Hybrid Molecules. *Appl. Phys. Lett.* **2012**, *101*, 093306.

(10) Nakagawa, T.; Ku, S. Y.; Wong, K. T.; Adachi, C. Electroluminescence Based on Thermally Activated Delayed Fluorescence Generated by a Spirobifluorene Donor−Acceptor Structure. *Chem. Commun.* **2012**, *48*, 9580−9582.

(11) Méhes, G.; Nomura, H.; Zhang, Q.; Nakagawa, T.; Adachi, C. Enhanced Electroluminescence Efficiency in a Spiro-Acridine Derivative through Thermally Activated Delayed Fluorescence. *Angew. Chem., Int. Ed.* **2012**, *51*, 11311−11315.

(12) Tanaka, H.; Shizu, K.; Miyazaki, H.; Adachi, C. Efficient Green Thermally Activated Delayed Fluorescence (TADF) from a Phenoxazine−Triphenyltriazine (PXZ−TRZ) Derivative. *Chem. Commun.* **2012**, *48*, 11392−11394.

(13) Baldo, M. A.; Lamansky, S.; Burrows, P. E.; Thompson, M. E.; Forrest, S. R. Very High-Efficiency Green Organic Light-Emitting Devices Based on Electrophosphorescence. *Appl. Phys. Lett.* **1999**, *75*, 4.

(14) Tokito, S.; Iijima, T.; Tsuzuki, T.; Sato, F. High-Efficiency White Phosphorescent Organic Light-Emitting Devices with Greenish-Blue and Red-Emitting Layers. *Appl. Phys. Lett.* **2003**, *83*, 2459.

(15) Adachi, C.; A. Baldo, M.; Thompson, M. E.; Forrest, S. R. Nearly 100% Internal Phosphorescence Efficiency in an Organic Light-Emitting Device. *J. Appl. Phys.* **2001**, *90*, 5048.

(16) Kim, S. H.; Jang, J.; Lee, J. Y. High Efficiency Phosphorescent Organic Light-Emitting Diodes Using Carbazole-Type Triplet Exciton Blocking layer. *Appl. Phys. Lett.* **2007**, *90*, 223505.

(17) Im, Y.; Lee, J. Y. Above 20% External Quantum Efficiency in Thermally Activated Delayed Fluorescence Device Using Furodipyridine-Type Host Materials. *Chem. Mater.* **2014**, *26*, 1413−1419.

(18) Kim, B. S.; Lee, J. Y. Engineering of Mixed Host for High External Quantum Efficiency above 25% in Green Thermally Activated Delayed Fluorescence Device. *Adv. Funct. Mater.* **2014**, DOI: 10.1002/adfm.201303730.

(19) Cho, Y. J.; Yook, K. S.; Lee, J. Y. A Universal Host Material for High External Quantum Efficiency Close to 25% and Long Lifetime in Green Fluorescent and Phosphorescent OLEDs 2014, DOI: 10.1002/adma.201400347.

(20) Son, H. S.; Seo, C. W.; Lee, J. Y. Correlation of the Substitution Position of Diphenylphosphine Oxide on Phenylcarbazole and Device Performances of Blue Phosphorescent Organic Light-Emitting Diodes. *J. Mater. Chem.* **2011**, *21*, 5638−5644.

(21) Nakanotani, H.; Masui, K.; Nishide, J.; Shibata, T.; Adachi, C. Promising Operational Stability of High-Efficiency Organic Light-Emitting Diodes Based on Thermally Activated Delayed Fluorescence. *Sci. Rep.* **2013**, *3*, 2127.

(22) Jeon, S. O.; Jang, S. E.; Son, H. S.; Lee, J. Y. External Quantum Efficiency Above 20% in Deep Blue Phosphorescent Organic Light-Emitting Diodes. *Adv. Mater.* **2011**, *23*, 1436−1441.